ELSEVIER

Chemical Engineering Journal 79 (2000) 1–12

Chemical Engineering Journal

www.elsevier.com/locate/cej

Pareto design of fluidized bed dryers

M.K. Krokida*, C.T. Kiranoudis

Department of Chemical Engineering, National Technical University of Athens, GR 15780, Athens, Greece

Received 5 April 1999; received in revised form 3 December 1999; accepted 11 December 1999

Abstract

Most of the research efforts in the field of fluidized dryer design, focus on the evaluation of the appropriate structural and operational process variables so that total annual plant cost involved is optimized. However, the increasing need for dehydrated products of the highest quality, imposes the development of new criteria that, together with cost components, determine the design rules for any drying process. Quality of dehydrated products is a complex resultant of properties characterizing the final products, where the most important one is color. Color is represented by three parameters: redness, yellowness and lightness. These three parameters of a dried product should deviate from that of its original material as little as possible. In this case, fluidized bed dryer design is a complex multi-objective optimization problem, involving the color deviation and the unit cost of final product as an objective vector and as constraints described in process models. The mathematical model of the dryer was developed and the fundamental color deterioration laws and critical financial parameters were determined for the fluidized bed drying process. In this paper, non-preference multi-criteria optimization methods were used and the Pareto-optimal set of efficient solutions was evaluated. An example for drying of sliced potato was studied in detail to demonstrate the design procedure, the process performance as well as the effectiveness of the proposed approach.

Keywords: Pareto design; Fluidized bed dryers; Multiobjective optimization; Mathematical modeling

1. Introduction

Process design chiefly aims at the determination of various sizing and operational variables involved in the mathematical model describing the process itself on technical and economic grounds. The evaluation of desired process variable values for each design effort is carried out by appropriately optimizing a suitable criterion chiefly on an economical nature. In the case of dryers, design has become an increasingly challenging problem which aims at the evaluation of the proper type of equipment, its associated flowsheet arrangement, its optimal construction characteristics and the operating conditions involved in the overall design. However, most design efforts in this field face problems of extreme difficulty related to the complex drying conditions that include many interconnected and opposing phenomena [1]. In addition, although numerous theories have been developed for modeling the drying processes, the thermophysical properties and transport coefficients in most models are only approximately known, producing inaccurate or erroneous results on large scale industrial applications [2–7].

Transferring mathematical programming analysis to this area of dryer design revealed several issues regarding sensitivity analysis with respect to process variables with a direct impact on dryer performance, as well as consideration of the actual operational performance under variable production conditions and selection of dryer type with respect to market and cost status. Several researchers have addressed all these diversified fields of simulation and design for fluidized bed dryers. Jumah and Mujumdar [8] give the outline of a computer program developed for the preliminary design of a fluidized bed dryer. It is based on correlations extracted from the literature and permits estimation of the energy consumption as well as the installed and operational cost. Maroulis et al. [9] developed a fluidized bed dryer simulator based on a mathematical model describing heat and mass transfer within the dryer. The model incorporates empirical equations for the drying constant and the multi-dispersed particle phase residence time. The experience from the application of the simulator has been proved to be important for the flexible operation of an existing industrial fluidized bed dryer. Kiranoudis et al. [10] developed a mathematical model for fluidized bed dryers. Design procedures aimed at the determination of optimum sizing and operational characteristics were carried out by appropriately optimizing the

* Corresponding author.
E-mail address: maroulis@chemeng.ntua.gr (M.K. Krokida)

1385-8947/00/$ – see front matter
PII: S1385-8947(00)00140-6

total annual cost for a given product capacity. Kiranoudis et al. [11] compared explicitly design results by evaluating optimum configurations for a wide range of production capacity values. Once the dryer sizing variables were defined, its operational performance was evaluated by comparing the optimal operating cost versus production capacity for predefined optimal design structures.

On the above-mentioned analysis, dryer design involves solely variations over plant profit or cost (when production capacity was given) as an objective function. The increasing need for dehydrated products of highest quality standards, requests the development of new criteria that, together with cost, determine new design rules. Quality of dehydrated products is a complex resultant of properties characterizing the final products, in which the most important one is color. Color is determined as a three-parameter resultant, whose values for products undergone drying should deviate from the corresponding ones of natural products, as little as possible [12]. In this case, dryer design is a complex multi-objective optimization problem involving an objective function of unit cost and color deviation vector and constraints derived from the process mathematical model.

In this work, we deal with the fluidized dryer design problem based on product quality criteria combined with cost. In this case, the optimal construction and operational process variables are evaluated by appropriately optimizing the product color degradation vector with unit product cost simultaneously subject to constraints imposed by model equations. Non-preference Pareto-optimization methodology is adopted and appropriately analyzed. The full set of efficient optimal solutions for the problem is evaluated and the effect of optimal design variables on process construction and operational variables is investigated for a typical industrial dryer design concerning sliced potatoes.

2. Mathematical modeling of fluidized bed dryers

Industrial fluidized bed dryers are the most popular family of dryers for drying agricultural and chemical products in dispersion or multi-dispersion state. In continuous industrial fluidized bed dryers, the particular solid phase is completely dispersed in a vertically flowing gas stream as a consequence of the buoyancy effect of the gas. Due to the agitation in the fluidized bed, good mixing of the solid phase is usually achieved. Moreover, the turbulent activity in the bed, produces high rates of heat transfer between gas and solid phases and results in uniform solids and gas temperature throughout the dryer. Fluidization takes place when the gas superficial velocity varies between two extreme values corresponding to fluidization and entrainment phenomena. The particular gas velocities in this case are particularly influenced by particle density and size. The dryer is equipped with an individual heating utility and fans for air recirculation through the product. Steam-operated heat exchangers are typically used for heating air that on entering the dryer

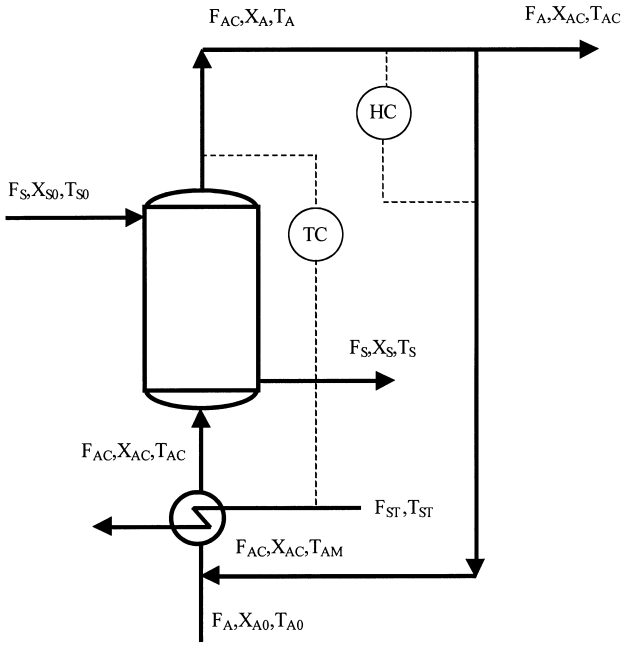

Fig. 1. Industrial fluidized bed dryer and its control facilities.

is mixed with the recirculation air at a point below the heat exchange units. It is a common practice that within the dryer interior, temperature and humidity of the air-drying stream as well as its temperature diminution through the fluidized solid bed are controlled. In this case, the final control elements are the steam valve, the drying air stream dampers and air flowrate through the fans, that regulate the exchanged heat rate at dryer heat exchangers, the flow rate of air streams within the dryer and the drying rate, respectively. A typical flowsheet with a sketch of the dryer, as well as the arrangement of its overall control facilities, is presented in Fig. 1.

The mathematical model of the fluidized bed dryer involves heat and mass balances of air and product streams, as well as heat and mass transfer phenomena that take place during drying. The system of equations generated is subject to thermodynamic and construction constraints that must be taken into consideration. In particular, the overall humidity balance in the dryer including recycle and its individual tank excluding recycle, respectively, is given by the following equations:

$$F_S(X_{S0} - X_S) = F_{AC}(X_A - X_{AC}) \quad (1)$$

$$F_S(X_{S0} - X_S) = F_A(X_A - X_{A0}) \quad (2)$$

The corresponding heat balances assuming negligible heat losses, are given as follows:

$$F_{AC}(h_{AC} - h_A) = Q - F_A(h_A - h_{A0}) \quad (3)$$

$$F_{AC}(h_{AC} - h_A) = F_S(h_S - h_{S0}) \quad (4)$$

Heat and mass transfer phenomena during drying are complex and their solution demands considerable computational time. They involve coupled transfer mechanisms,

both within the solid and the gas phase. In this case, a simplified mathematical model is considered. This version has an exponential form and contains a phenomenological mass transfer coefficient, termed as the drying constant. The drying constant chiefly accounts for mass diffusion within the solid phase, but also embodies boundary layer phenomena when it is considered to be a function of all process variables affecting drying. Sufficient accuracy is combined with sufficiently low computational time. With these assumptions, mass transfer is expressed by the following equation:

$$X_S = X_{SE} + (X_{S0} - X_{SE}) \exp(-k_M t_R) \quad (5)$$

The retention time within the fluidized bed dryer is chiefly influenced by process hydrodynamics and particle size distribution. A detailed account on this issue can be found in Maroulis et al. [9]. For the purpose of this study that is far beyond giving a detailed account of the single objective optimization case, uniform particle size distribution was taken into consideration. Heat transfer is chiefly controlled by the heat transfer coefficient at the air boundary layer. For the purpose of developing the particular mathematical model, it is assumed that the heat transfer coefficient takes a value high enough to allow the product stream leaving the dryer to be in thermal equilibrium with the air stream leaving the solid phase. This assumption removes the need for an unnecessary differential equation, which would not improve the model greatly. On the basis of the above, heat transfer within the dryer is expressed by means of the following equation:

$$T_S = T_A \quad (6)$$

The air water activity of the drying air stream is calculated by the basic equation of a psychrometric model as follows:

$$a_{WC} = \frac{X_{AC} P}{(\lambda_B + X_{AC}) P^S} \quad (7)$$

Drying air flowrate within the dryer is given by the following equation expressing basic aerodynamics within the dryer:

$$F_{AC} = \rho_{AC} A V_{AC} \varepsilon \quad (8)$$

In this relation, air flowrate is given as a function of the porosity of the fluidized bed. The corresponding bed height is given by the following equation:

$$H = \frac{F_S(1 + X_{S0}) t_R}{\rho_S A (1 - \varepsilon)} \quad (9)$$

which is an alternative expression for solids holdup in the dryer. The gas flow through the fluidized bed, can be treated as an equivalent one through a porous body with given porosity [13]. It is suggested for the condition of incipient fluidization, but it can safely be used for all the fluidization region since pressure drop remains constant from fluidization up to entrainment [14]. Thus, pressure drop along the dryer is given by the following equation:

$$\Delta P = (\rho_S - \rho_{AC})(1 - \varepsilon) H g \quad (10)$$

Heat balances at the heat exchanger section of the dryer are given as follows:

$$Q = F_{ST} \Delta H_S \quad (11)$$

$$Q = U_{ST} A_{ST} \frac{T_{AC} - T_{AM}}{\ln((T_{ST} - T_{AM})/(T_{ST} - T_{AC}))} \quad (12)$$

The temperature of the mixed recirculation and fresh air streams can be calculated by means of the enthalpy balance expressed by the following equation:

$$F_{AC} h_{AM} = F_A h_{A0} + (F_{AC} - F_A) h_A \quad (13)$$

The electrical power consumed by the operation of the fans is expressed by the following equation:

$$E = \Delta P F_{AC} \quad (14)$$

The temperature diminution of the drying air stream in passing through the solid particles is given by the following equation:

$$\Delta T = T_{AC} - T_A \quad (15)$$

The temperature diminution of the drying air stream in passing through the solid particles fluidized phase, should not exceed a maximum value that would guarantee uniform drying throughout dryer, because it prevents creation of axial mass and temperature gradients within the solid particles. This is expressed by the following inequality:

$$0 \leq \Delta T \leq \Delta T^{max} \quad (16)$$

Furthermore, thermodynamics dictate that the material moisture content of the product stream on leaving the dryer should be greater than the corresponding moisture content at equilibrium imposed by the air operating conditions in the dryer, as proposed by the following relation:

$$X_S \geq X_{SE} \quad (17)$$

Fluidized bed porosity is given by the Todes equation, involving the dimensionless Reynolds and Archimedes numbers and is recommended for the related calculations for the entire fluidization region [15,16]

$$\varepsilon = \left(\frac{18\,\mathrm{Re} + 0.36\,\mathrm{Re}^2}{\mathrm{Ar}} \right)^{0.21} \quad (18)$$

$$\mathrm{Re} = \frac{V_{AC} \rho_{AC} d_P}{\mu_{AC}} \quad (19)$$

$$\mathrm{Ar} = \frac{(\rho_S - \rho_{AC}) g \rho_{AC} d_P^3}{\mu_{AC}^2} \quad (20)$$

Fluidization is guaranteed if drying air stream velocity varies between two extremes. Incipient fluidization velocity calculated by the following equation, is derived from the theory of free settling:

$$V_{AC}^{min} = \left[\frac{4}{3} \frac{d_P (\rho_S - \rho_{AC})}{\rho_{AC}} \frac{1}{(0.4 + 24/\mathrm{Re} + 4/\mathrm{Re}^{1/2})} \right]^{1/2} \quad (21)$$

Strumillo and Kudra [16] list over 20 equations for the determination of this variable as suggested from various researchers. Romankov and Rashkovskaya [17] recommended the following equation for the calculation of entrainment gas velocity:

$$V_{AC}^{max} = V_{AC}^{min}\left(11.75 - \frac{0.1046}{1 + 0.00373\,Ar^{0.6}}\right) \quad (22)$$

The economic evaluation of the dryer is based upon the determination of its total annual cost. The corresponding capital cost is affected by the total dryer area (cross section and peripheral), the area of heat exchangers and the installed power of the fans involved. All capital cost components obey economy of scale laws, i.e. increase in the unit size with respect to its characteristic dimensions will contribute reduced additional capital cost, per unit of size

$$C_{CP} = \alpha_D A_T^{\eta_D} + \alpha_F E^{\eta_F} + \alpha_{ST} A_{ST}^{\eta_{ST}} \quad (23)$$

The operational cost of the plant involves thermal and electrical energy, consumed by the heat exchangers and fans, respectively

$$C_{OP} = c_E E + c_{ST} F_{ST} \quad (24)$$

On the basis of the above, the total annual cost of the plant can be expressed by means of the following equation:

$$C_T = eC_{CP} + t_{OP} C_{OP} \quad (25)$$

The unit cost of the final product can be readily calculated by means of the following equation:

$$c^* = \frac{C_T}{F_S(1 + X_S)t_{OP}} \quad (26)$$

Product color changes measured by tristimulus reflectance colorimetry can be used to predict both chemical and quality changes in a food system. The Hunter color parameters have previously proved valuable in describing visual color deterioration and providing useful information for quality control in final products [12]. The rate of color changes for the *i*th index of each of the three Hunter color parameters (namely redness, α, yellowness, b, and lightness, L) can be expressed by the following first order kinetic model [12]:

$$\Delta C^i = (C_E^i - C_0^i) + (C_0^i - C_E^i)\exp(-k_C^i t_R) \quad (27)$$

The properties and transfer coefficients involved in the mathematical model of the dryer are generally considered to be functions of the process variables. Specific enthalpies of product and air streams are taken to be linear functions of temperature and material moisture content, since the corresponding specific heats of solid particles, dry air, water, and vapor are assumed to be constant within the desired temperature range [18]

$$h_S = c_{PS} T_S + X_S c_{PW} T_S \quad (28)$$

$$h_A = c_{PA} T_A + X_A(\Delta H_0 + c_{PV} T_A) \quad (29)$$

Equilibrium of water between the solid and the gas phase is described by the process desorption isotherms, modeled by means of the theoretically determined GAB equation, which sufficiently describes the equilibrium data for a wide range of products used in the dehydration process [19]

$$X_{SE} = \frac{X_M C T a_W}{(1 - K a_W)([1 - (1 - C)K a_W]} \quad (30)$$

$$C = C_0 \exp\left(-\frac{\Delta H_C}{RT_S}\right) \quad (31)$$

$$K = K_0 \exp\left(-\frac{\Delta H_K}{RT_S}\right) \quad (32)$$

The drying constant as a function of drying air operating conditions as well as the characteristic dimension of material particles is given by the following empirical equation [1]:

$$k_M = k_0 T_{AC}^{k_1} X_{AC}^{k_2} V_{AC}^{k_3} d_P^{k_4} \quad (33)$$

Water vapor pressure can be calculated by means of the empirical Antoine equation given below:

$$P^S = \exp\left(A_1 - \frac{A_2}{A_3 + T_S}\right) \quad (34)$$

The latent heat of vaporization of water is given by the Clausius–Clapeyron equation that follows, which makes use of the previous vapor pressure equation:

$$\Delta H_S = -R\frac{d(\ln P^S)}{d(1/T_{ST})} \quad (35)$$

Air density can be calculated by assuming ideal gas behavior for air streams, as follows:

$$\rho_{AC} = \frac{P}{M_A R T_{AC}} \quad (36)$$

The effect of drying air operating conditions on color kinetics is introduced through its effect on the color degradation equilibrium value and rate constant for the *i*th parameter of color, as follows [12]:

$$C_E^i = C_{E0}^i T_{AC}^{n_T^i} X_{AC}^{n_X^i} \quad (37)$$

$$k_C^i = k_{C0}^i T_{AC}^{m_T^i} X_{AC}^{m_X^i} \quad (38)$$

Eqs. (1)–(38) constitute the mathematical model of the fluidized bed dryer. They involve three design variables that must be optimally set so that the complete dryer mathematical model is solved; namely drying air stream temperature and humidity, $T_{AC}$and X_{AC}, and the drying air stream temperature diminution through the fluidized bed dryer, ΔT. These variables can represent the process in a more straightforward way, due to their explicit meaning, and all other variables involved in the overall process model can be calculated accordingly.

3. Pareto optimization

Multi-objective optimization extends optimization theory by permitting multiple objectives to be optimized simultaneously. It is known by various names which include Pareto optimization, vector optimization, efficient optimization and multi-criteria optimization. The solutions are referred to as Pareto optima, vector maxima, efficient points, non-inferior and non-dominated solutions. In all cases, multi-objective optimization is regarded as a mathematical process seeking a consensus in which many objectives are balanced so that the improvement of any single objective will result in a negative impact on at least one other objective. Such a system of objectives is said to be Pareto optimal at any point for which this is true. The Pareto-optimal solution is not unique (unlike the single optimization case), but is a member of a set of such points which are considered equally good in terms of the vector objective. This space may be viewed as a space of compromise solutions in which each objective could be improved, but if it were, it could be improved at the expense of at least one other objective. Geometrically, a Pareto-optimal point corresponds to a saddle point in the space formed by the objectives as coordinates. Infinitesimal motion away from the Pareto-optimal point increases the value of at least one objective as coordinate.

Mathematically speaking, multi-objective optimization is an extension of ordinary single-objective optimization where the objective function is a vector of functions over the feasible space of decision variables. A superior solution of the optimization problem is the set of all feasible points where there does not exist another feasible point performing better in all components of the objective vector [20]. Typically, however, at least two of the objectives are conflicting in nature. For this reason, a superior solution to the multi-objective optimization problem rarely exists. In problems such as these, the decision-maker is interested in finding efficient (also known as non-dominated or non-inferior) solutions. An efficient solution is the set of all feasible points where there does not exist another feasible point which does at least as well on every single objective, and better on at least one objective [20]. In other words, a feasible solution is non-inferior if there does not exist another feasible solution that will yield an improvement in one objective without causing degradation in all other objectives. For all non-inferior solutions the decision-maker will always consider how much of one objective is able to be given up for how much improvement in some other objectives. A superior solution (if it exists) is always an efficient solution, whereas an efficient solution is not necessarily a superior solution.

Typically, the feasible solutions to the multi-objective optimization problem are only partially ordered by the 'more is better' assumption. Hence, in most cases, there will be many efficient solutions. One of these efficient solutions will be preferred by the decision-maker, in terms of its outcome, at least as much as any other feasible solution. However, determining what the solution is, assuming the existence of at least two efficient solutions with different outcomes, requires further information from the decision-maker concerning his preferences. One way of expressing this information is through the use of a value function over the multiple objectives of the problem. In essence, this procedure recasts the multiple objective problems into one involving a single objective, that is to say optimization of the value function. Two mappings are involved in this case; one from the decision variable space to the objective space and a second from the objective space to the value space. Solving this type of problem means finding the solution that optimizes the value function over all feasible solutions. Such a solution is called a best compromise solution, in the sense that is typically a compromise among the problem's various objectives. Under the above-mentioned concepts, if a value function could be easily found for each and every multi-objective mathematical problem, there would be no need for dealing with such kind of problems since they would become a trivial case of a general single-objective optimization problem. However, a value function is often very difficult to specify for a particular decision-maker or a group of decision-makers. But, assuming the existence of more than one efficient solution, at least some information can be obtained regarding the decision-maker's preference structure in order to find a best compromise solution. Hence, in addition to an optimization scheme, some procedure to obtain this preference information is required. Generally, solution techniques for multi-objective mathematical programming problems can be classified according to the timing of the requirements of the preference information versus the optimization. In particular, there are three different approaches depending on the articulation of the decision-maker's preference function [20]

- Prior to the optimization (a priori articulation of preferences).
- During, or in sequence with, the optimization (progressive articulation of preferences).
- After the optimization (a posteriori articulation of preferences).

The last case requires the determination of the complete set of non-inferior solutions before selecting a compromise point. In this work, we will adopt this last case that actually corresponds to a non-preference procedure. In this way, by evaluating the complete efficient solution space we can leave the choice of compromise to ad-hoc process experts.

4. Pareto optimization of fluidized bed dryers

On the basis of the above, a design strategy for the specific dryer type under product quality constraints can be postulated. Given a specified product with a predefined flowrate, to be dried from an initial to a desired moisture content level, under constraints imposed by thermodynamics and construction, the following must be determined:

- The appropriate sizing of the equipment (construction characteristics).

- The best set points of controllers (operating conditions).

The Pareto-dryer design problem which corresponds to the above-mentioned postulation and which strives for the determination of optimal process variables so that product quality of the final product is optimally weighted against unit product cost, can be formulated into a multi-objective optimization non-linear mathematical programming problem where the vector of product color deterioration parameters and the unit product cost should be minimized subject to process model constraints, as follows:

$$\min_{T_{AC}, X_{AC}, \Delta T} (\Delta\alpha, \Delta b, \Delta L, c^*) \tag{39}$$

The proposed methodology was applied to the design of a dehydration plant that treats 200 t per year db of sliced potato, on a 2000 h per year basis (i.e. 100 kg/h db). The raw material is to be dried in the form of cubes cut in 10 mm size, with initial material moisture content of 5 kg/kg db. The desired dried product material moisture content is 0.05 kg/kg db. Fresh air is available with a moisture content at 0.01 kg/kg db and 25°C cold conditions, typical atmospheric conditions for Greece. Uniform drying is achieved by not allowing drying air temperature diminution through the fluidized bed to exceed a value of 10°C. The cost of the fluidized bed tank is US$ 1600/m^2 increased with a power law of 0.75 as total dryer area varies. Heat exchangers and fans add a capital cost of US$ 480/m^2 and US$ 500/kW h, increased by 0.7 and 0.3 laws respectively. Heat exchangers used are of the plate type for heating air. Steam is available at 150°C and its unit cost is 0.2 c/kg, while electrical energy costs 8 c/kW h. The capital cost will be paid off within a period of 5 years. Economic figures refer to the Greek market for the year 1998.

The way in which process decision variables affect each one of the color objective vector components and for the specific product studied, is given in Fig. 2. Krokida et al. [12] have shown that the Hunter Lightness parameter is in fact unaffected by the entire process. As a consequence, the deviation of this component value throughout drying is negligible and, therefore, we will not take it into consideration for the evaluation of the optimal objective vector. The process variables that affect the remaining two color parameters (redness and yellowness) are the drying air conditions (temperature and humidity) as well as the corresponding drying time. Redness deviation increases as drying temperature increases for the same air humidity level, while the completely inverse phenomenon takes place for the case of yellowness deviation. The temperature effect is more intense in the case of redness deviation regarding the equilibrium values. Redness deviation increases as air humidity decreases for the same value of air temperature while, once again, the opposite phenomenon occurs for yellowness deviations. The humidity effect is more intense in the case of redness deviation regarding the equilibrium values, even more intense than in the case of temperature. Redness deviation kinetics are characterized by greater time constants with respect to yellowness deviations. Clearly, redness deviations will reach the equilibrium value imposed by drying air conditions slower

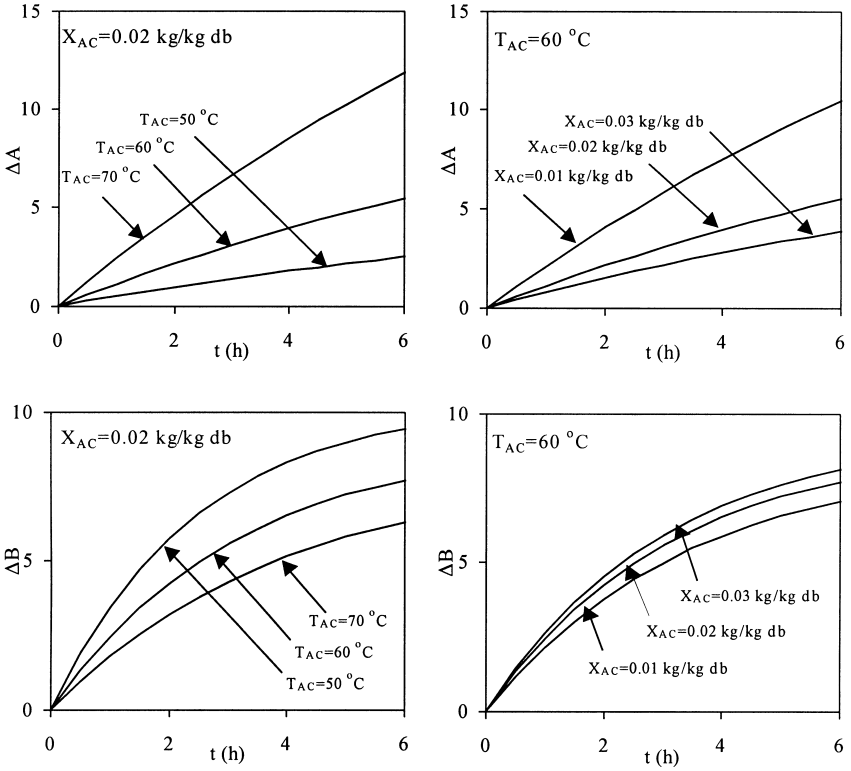

Fig. 2. Effect of process variables on color parameters.

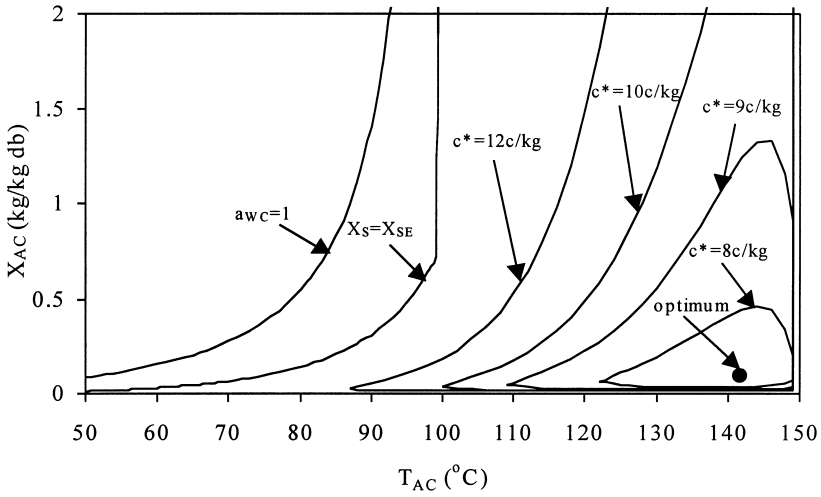

Fig. 3. Unit cost objective contours.

than the case of yellowness deviations. This in principle different behavior of color parameters during drying characterizes their optimality behavior when they are combined with process equations within the framework of multi-objective optimization.

A convenient way of approaching multi-objective simultaneous optimization for the entire process would be to examine each single-objective optimization separately. To be more specific, let us focus in each of the three objectives and optimize each one separately under a single-objective optimization schema. A global optimum was found for unit cost at air conditions 0.097 kg/kg db and 141.7°C, corresponding to an objective vector of (19.772, 0.241) for color and 7.29 c/kg db for unit cost. The unit cost contours of the process are given in Fig. 3. In this figure, several characteristic optimization curves are gathered, which is basically the psychrometric chart corresponding to drying air conditions; namely, the air water saturation curve (water activity equals to one), the constraint imposed by thermodynamics through Eq. (30) and the lower line limits the objective space to drying air humidity values greater than that of fresh air. In the same sense single-objective optimization contours for the color parameter vector are given in Fig. 4. A global optimum was found for redness deviation at air conditions 0.366 kg/kg db and 95.22°C, corresponding to an objective vector of (2.178, 2.578) and at unit cost value of 16.850 c/kg db. On the other hand no optimal value could be found for yellowness deviation since even smaller values could be obtained as temperature approached infinity and humidity was reaching fresh air values, an indication of functional strict monotony for the entire range of objective space. The difference between these two last objectives' behavior is definitely attributed to the different time constant related to color deterioration kinetics. Redness characterized by a larger time constant reaches its equilibrium value more slowly and as drying air conditions approach values in the vicinity of yellowness curve where outlet product material moisture content reaches equilibrium. Therefore an infinite drying time is implied for these values, an abrupt movement of this variables takes place and, as a consequence, a global optimum is formed. This is definitely not the case for yellowness deviations, where the kinetic time constant is lower and equilibrium is reached faster. In all cases, the optimal value for temperature diminution was the one of the constraint in Eq. (16).

Let us depict this behavior geometrically in the objective space formed by the two components of air condition (drying air temperature and humidity), as the third decision variable seems to be unaffected by the optimization procedure and for the case of the one color component (redness) and unit cost of the process. Global optimum for redness deviations as well as the corresponding redness deviation contour estimated for redness deviation values of 5 are also given in Fig. 5. An additional curve is a constant unit cost curve calculated for unit cost constant value of 9 c/kg db. Clearly, the form of both curves indicate global optimal objectives for the specific corresponding objective functions and we therefore expect closed curves for the single-optimization problems, as we have already mentioned. These curves although considered as random contours, were appropriately chosen to show something even more interesting. These curves have only one point of contact, in other words contour slopes at that point are the same, or the corresponding function derivatives are equal. This unique point can be easily shown to be a Pareto-optimal point of the multi-objective optimization problem. In fact, for this point there does not exist another feasible point which does at least as well on both single objectives, and better on at least one of the two. For this point, it can be easily shown using differential geometry that

$$\det\begin{bmatrix} \partial(\Delta\alpha)/\partial T_{AC} & \partial(\Delta\alpha)/\partial X_{AC} \\ \partial(c^*)/\partial T_{AC} & \partial(c^*)/\partial X_{AC} \end{bmatrix} = 0 \quad (40)$$

The locus of all decision points fulfilling Eq. (40) is the Pareto-optimal curve given in this figure and this is the complete set of Pareto-optimal solutions for the specific

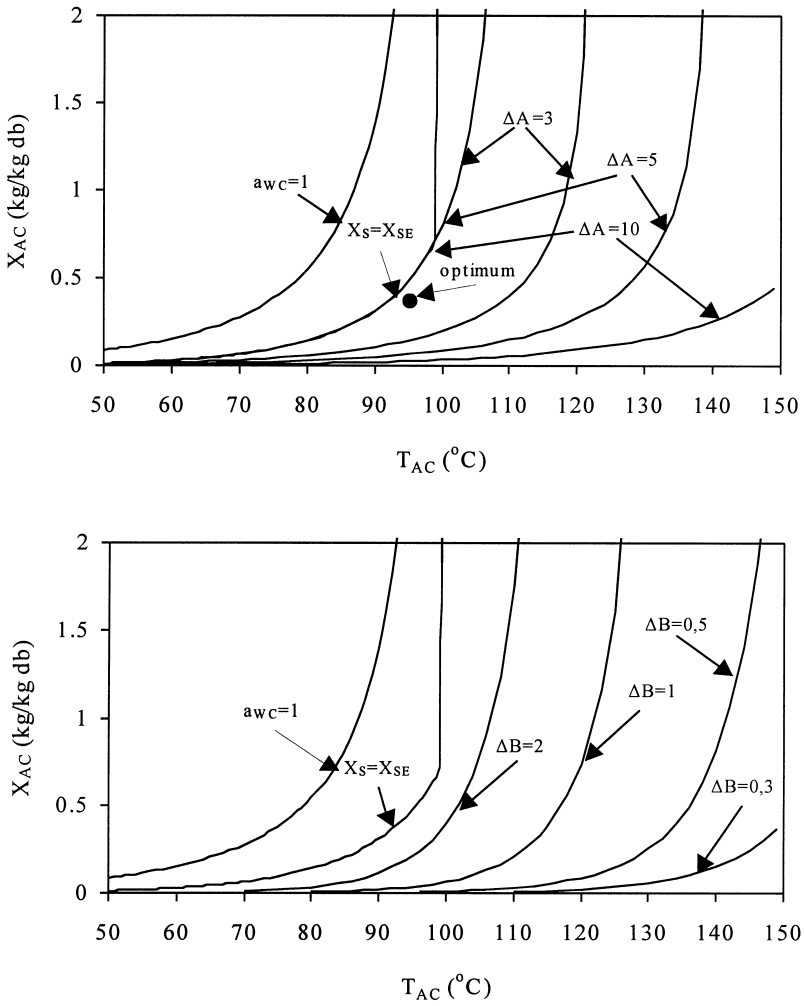

Fig. 4. Color parameters objective contours.

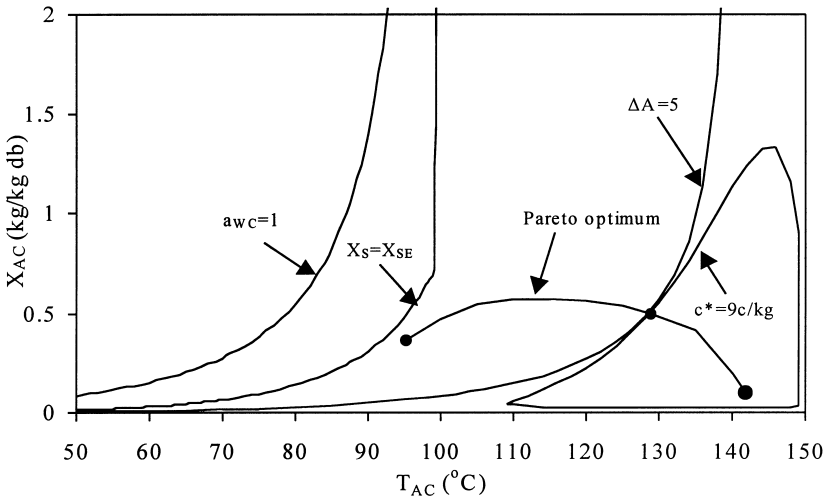

Fig. 5. Pareto-optimization procedure.

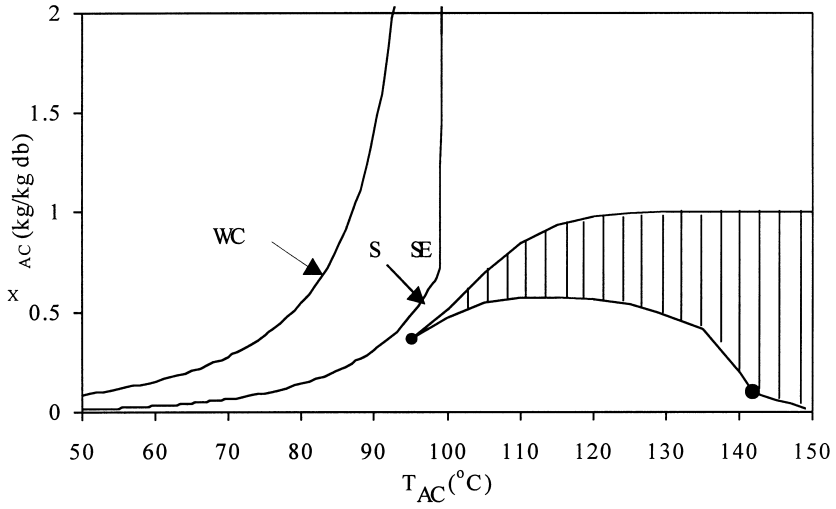

Fig. 6. Pareto-optimal set for fluidized dryers.

sub-problem studied. Obviously, the decision-maker will search for his compromise solutions within the single-dimensional range of this curve. The Pareto-optimal solution of the multi-objective optimization sub-problem discussed is given for the two-dimensional objective space in the curve of Fig. 5. This figure clearly shows the trade-offs between redness and unit cost which should be taken into account by decision makers.

The above-mentioned conclusions were obtained by considering only two components of the optimization vector. Clearly, similar Pareto-optimal curves can be derived when considering the other two pairs on their own. This procedure yields the envelope of the shaded area of Fig. 6. For these curves, the following condition hold:

$$\det\begin{bmatrix} \partial(\Delta\alpha)/\partial T_{AC} & \partial(\Delta\alpha)/\partial X_{AC} \\ \partial(\Delta b)/\partial T_{AC} & \partial(\Delta b)/\partial X_{AC} \end{bmatrix} = 0 \quad (41)$$

$$\det\begin{bmatrix} \partial(c^*)/\partial T_{AC} & \partial(c^*)/\partial X_{AC} \\ \partial(\Delta b)/\partial T_{AC} & \partial(\Delta b)/\partial X_{AC} \end{bmatrix} = 0 \quad (42)$$

The actual Pareto-optimal space of the entire four-component multi-objective design problem is the shaded area of Fig. 6. Obviously, the decision-maker will search for his compromise solutions within the two-dimensional space. Steam temperature is an important process variable that affects the unit cost and therefore the Pareto-optimal space of objectives. The Pareto-optimal space for the entire multi-objective optimization problem as a function of steam temperature is given in Fig. 7. The Pareto-optimal curve for the two-color component vector remains the same since it is not affected by the steam temperature (solely affected by process variables). On the other hand, both two-component Pareto sets involving cost are indeed affected by steam temperature and they are responsible for the different extend of the

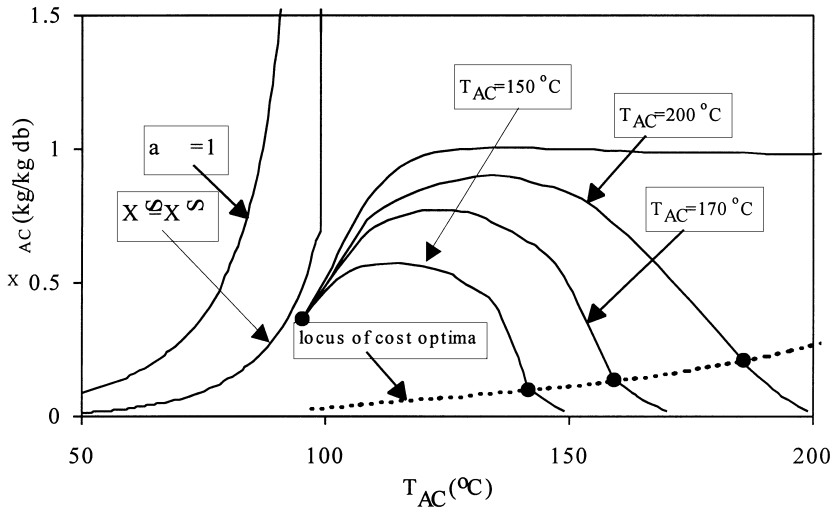

Fig. 7. Effect of steam temperature on Pareto-optimal region.

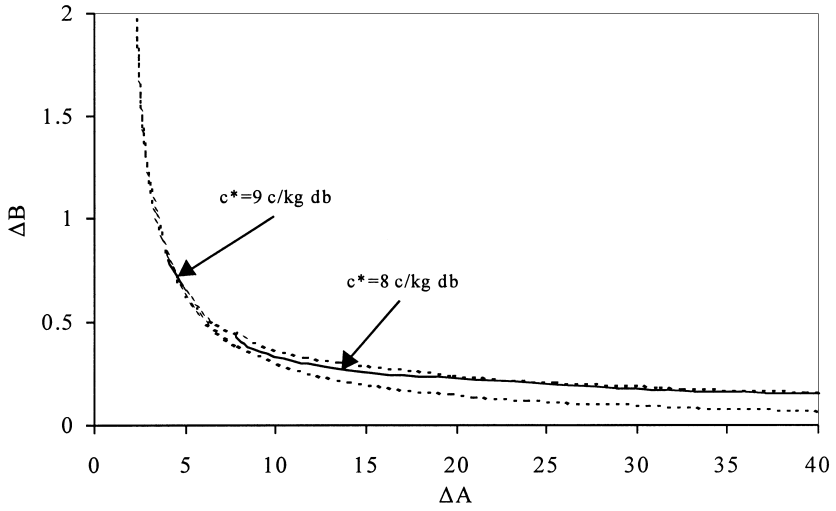

Fig. 8. Pareto-optimal objective space.

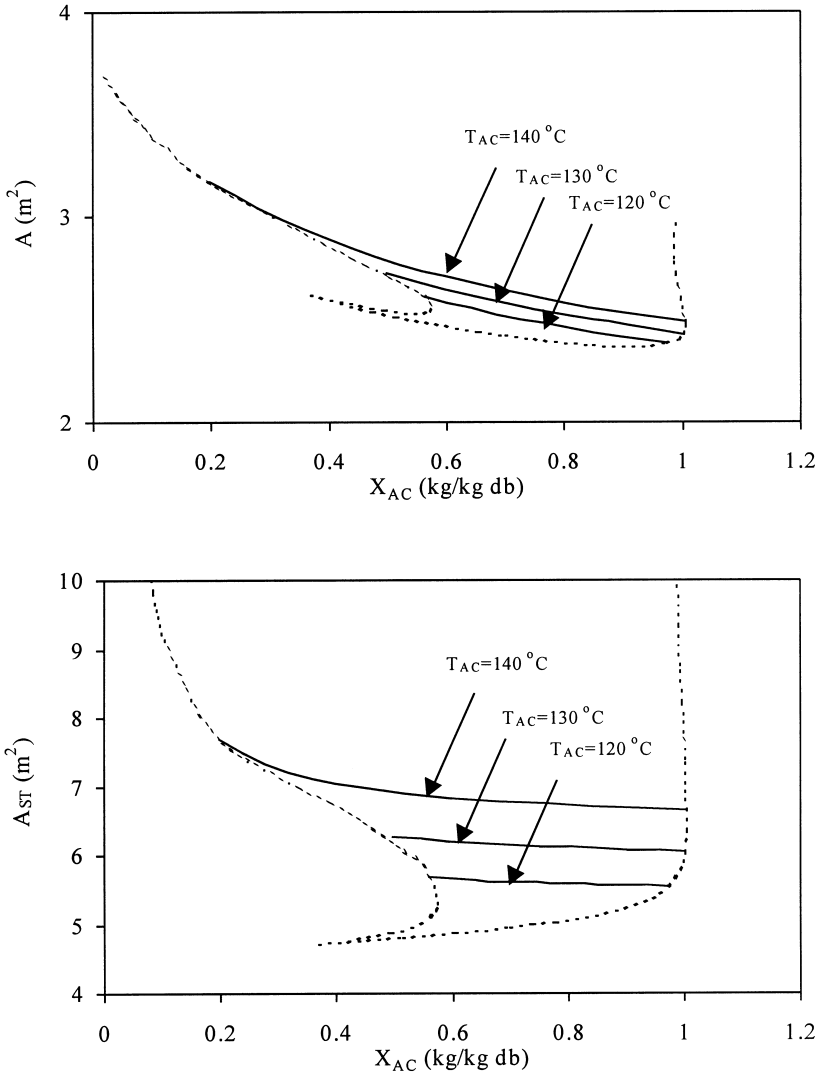

Fig. 9. Pareto-optimal process construction variables.

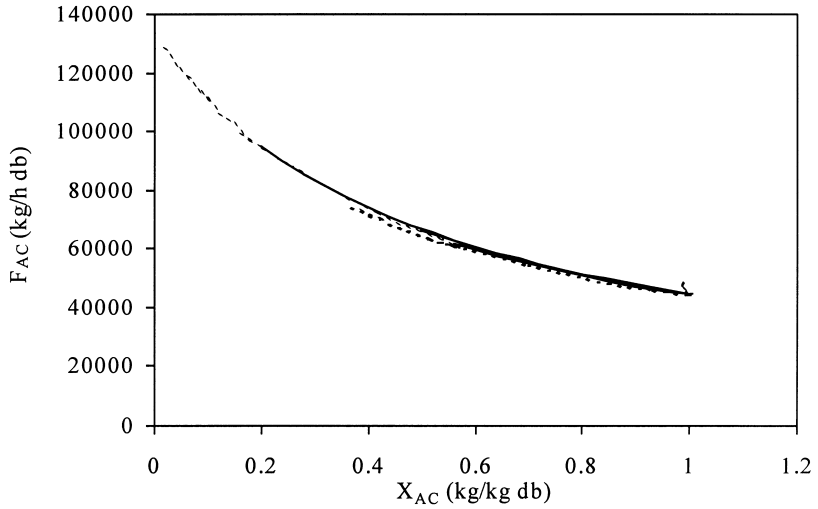

Fig. 10. Pareto-optimal operational variable.

entire Pareto space of this process. The different Pareto regions are appropriately depicted in this figure as steam temperature varies. In the same figure the locus of global unit cost optima using steam temperature as the independent variable is given. The shape of this curve definitely affects the curvature of the Pareto space of the optima.The complete process objective space is given in Fig. 8. In this particular figure, unit cost contours are given confined by Pareto-optimal space for the remaining color components space boundaries. If we reduce our demand for unit cost above 8 c/kg db, optimal yellowness deviation values can be achieved for values lower than 0.5, while redness deviation in this case can be any value above around 5. We can obtain lower unit cost designs for fluidized beds examined, while redness deviation is kept to the minimum, but in this case, yellowness deviation is far from its optimal value.

The way that certain process variables (construction and operational) vary with the Pareto-optimal solution obtained is given in Figs. 9 and 10. We observe similar behavior regarding the heat exchanger and fluidized bed area, while for drying air stream flowrate, the Pareto solutions are strictly close and are not affected by drying air stream temperature. Again, the appropriate design could be easily determined regarding the desire of the decision-make over the complete set of derived Pareto-optimal curves.

5. Conclusions

Fluidized bed dryer design based on combined cost and product quality criteria is demanded by the increasing need for dehydrated products of highest quality standards. This problem can be appropriately formulated into a multi-objective non-linear mathematical programming problem where the final product color parameter vector together with unit cost is optimized subject to constraints imposed by thermodynamics, construction, and modeling. Non-preference multi-criteria optimization methods can be used and the Pareto-optimal set of efficient solutions can be evaluated as the single-dimensional locus of decision variables' points fulfilling a specific analytical relationship. Decision-making can therefore be based on the Pareto-optimal solution obtained.

6. Nomenclature

A	dryer cross-section area (m^2)
Ar	Archimedes number
A_T	dryer total peripheral and cross section area (m^2)
A_j	parameter of Eq. (34) where j=1, 2, 3
A_{ST}	heat exchanger area (m^2)
a_{WC}	drying air stream water activity
b	yellowness
C^i	color value of parameter i
C	parameter of Eq. (30)
c^*	unit cost of final products ($/kg db)
C_0	parameter of Eq. (27)
C_{CP}	capital cost ($)
c_E	unit cost of electricity ($/kW h)
C^i_E	equilibrium value of parameter i
C_{E0}	parameter of Eq. (37)
C_{OP}	operational cost ($/h)
C_0	parameter of Eq. (31)
C^i_0	initial value of parameter i
c_{PA}	specific heat of air (kJ/kg K)
c_{PS}	specific heat of solid (kJ/kg K)
c_{PV}	specific heat of water vapor (kJ/kg K)
c_{PW}	specific heat of water (kJ/kg K)
c_{ST}	unit cost of steam ($/kg)
C_T	total annual cost ($ per year)
db	dry basis
d_P	particle diameter (m)
E	electrical power consumed at dryer fans (kW)

e	percentage of capital cost on annual rate
F_A	fresh air stream flowrate (kg/h db)
F_{AC}	drying air stream flowrate (kg/h db)
F_S	product stream flowrate (kg/h db)
F_{ST}	steam flowrate (kg/h)
g	gravitational constant (m/s^2)
H	bed height (m)
h_A	specific enthalpy of outlet air stream (kJ/kg)
h_{A0}	specific enthalpy of fresh air stream (kJ/kg)
h_{AC}	specific enthalpy of drying air stream (kJ/kg)
h_{AM}	specific enthalpy of mixed recirculation and fresh air streams (kJ/kg)
K	parameter of Eq. (30)
K_0	parameter of Eq. (31)
k_j	parameter of Eq. (33) where j=0, ..., 4
K_C^i	rate of color deterioration constant of parameter i (1/h)
k_{C0}	parameter of Eq. (38)
k_M	drying constant (1/h)
L	lightness
M_A	molecular weight (kg/kg mol)
m_T, m_X	parameters of Eq. (38)
n_T, n_X	parameters of Eq. (37)
P	absolute pressure (kPa)
P^S	vapor pressure of water (kPa)
Q	heat exchanged at dryer heat exchangers (kW)
R	gas constant (kJ/kg K)
Re	Reynolds number
X_A	outlet air stream humidity (kg/kg db)
X_{A0}	fresh air stream humidity (kg/kg db)
X_{AC}	drying air stream humidity (kg/kg db)
X_S	outlet product stream material moisture content (kg/kg db)
X_{S0}	inlet product stream material moisture content (kg/kg db)
X_{SE}	equilibrium product stream material moisture content (kg/kg db)
t_{OP}	total operating time for dryer operation (h per year)
t_R	residence drying time (h)
T_A	outlet air stream temperature (°C)
T_{A0}	fresh air stream temperature (°C)
T_{AC}	drying air stream temperature (°C)
T_{AM}	mixed recirculation and fresh air stream temperature (°C)
T_S	outlet product stream temperature (°C)
T_{S0}	inlet product stream temperature (°C)
U_{ST}	overall heat transfer coefficient (kW/m^2 K)
V_{AC}^{max}	incipient fluidization velocity (m/s)
V_{AC}^{min}	entrainment fluidization velocity (m/s)
wb	wet basis

Greek letters

α	redness
α_D, α_F, α_{ST}	cost parameters of Eq. (23)
ΔH_S	latent heat of vaporization of water (kJ/kg)
ΔH_{S0}	latent heat of vaporization of water at reference temperature 0°C (kJ/kg)
ΔH_C	parameter of Eq. (31)
ΔH_K	parameter of Eq. (32)
ΔT	temperature diminution through particles (°C)
ΔT^{max}	maximum allowed temperature diminution through particles (°C)
ε	porosity
λ_B	water to air molecular weight ratio
η_D, η_F, η_{ST}	cost parameters of Eq. (23)
ρ_{AC}	drying air density (kg/m^3)
ρ_S	solid particle density (kg/m^3)
μ_A	viscosity (Pa s)

Symbols

Δ	deviation
det	determinant
i	index of color parameter

References

[1] C.T. Kiranoudis, Z.B. Maroulis, D. Marinos-Kouris, Drying Technol. 10 (1992) 1097–1106.
[2] C.T. Kiranoudis, Z.B. Maroulis, D. Marinos-Kouris, Drying Technol. 11 (1993) 1251–1270.
[3] C.T. Kiranoudis, Z.B. Maroulis, D. Marinos-Kouris, Int. J. Heat Mass Transfer 38 (1995) 463–480.
[4] C.T. Kiranoudis, Z.B. Maroulis, E. Tsami, D. Marinos-Kouris, Drying Technol. 15 (1997) 735–763.
[5] Z.B. Maroulis, C.T. Kiranoudis, D. Marinos-Kouris, J. Food Eng. 26 (1995) 113–130.
[6] D. Marinos-Kouris, Z.B. Maroulis, C.T. Kiranoudis, Drying Technol. 14 (1996) 971–1010.
[7] D. Marinos-Kouris, Z.B. Maroulis, C.T. Kiranoudis, Drying Technol. 16 (1998) 993–1026.
[8] R.Y. Jumah, A.S. Mujumdar, Drying Technol. 11 (1993) 831–846.
[9] Z.B. Maroulis, C. Kremalis, T. Kritikos, Drying Technol. 13 (1995) 1763–1788.
[10] C.T. Kiranoudis, Z.B. Maroulis, D. Marinos-Kouris, AIChE J. 42 (1996) 3030–3040.
[11] C.T. Kiranoudis, Z.B. Maroulis, D. Marinos-Kouris, Drying Technol. 15 (1997) 735–763.
[12] M.K. Krokida, E. Tsami, Z.B. Maroulis, Drying Technol. 16 (1998) 667–685.
[13] R.D. Marcus, L.S. Leung, G.E. Klinzing, F. Rizk, Pneumatic Conveying of Solids, Chapman & Hall, New York, 1990.
[14] S. Hovmand, Fluidized bed drying, in: A.S. Mujumdar (Ed.), Handbook of Industrial Drying, Marcel-Dekker, New York, 1995, pp. 195–248.
[15] M.E. Aerov, O.M. Todes, Hydrodynamic and Heat Transfer Principles of Apparatus with Fixed and Fluidized Beds, Khimiya, Leningrad, 1968.
[16] C. Strumilo, T. Kudra, Drying: Principles, Applications and Design, Gordon and Breach, New York, 1986.
[17] P.G. Romankov, N.B. Rashkovskaya, Drying in Suspension State, Khimiya, Leningrad, 1979.
[18] C.T. Kiranoudis, Z.B. Maroulis, D. Marinos-Kouris, J. Food Eng. 23 (1994) 375–396.
[19] C.T. Kiranoudis, Z.B. Maroulis, E. Tsami, D. Marinos-Kouris, J. Food Eng. 20 (1993) 55–74.
[20] G.W. Evans, Manage. Sci. 30 (1984) 1268–1282.